Lab on a Chip

Cite this: *Lab Chip*, 2012, **12**, 4644–4650

www.rsc.org/loc

PAPER

Inertial microfluidics in parallel channels for high-throughput applications

Jonas Hansson,[ab] J. Mikael Karlsson,[c] Tommy Haraldsson,[c] Hjalmar Brismar,[ad] W. van der Wijngaart[c] and Aman Russom*[ab]

Received 8th March 2012, Accepted 24th July 2012
DOI: 10.1039/c2lc40241f

Passive particle focusing based on inertial microfluidics was recently introduced as a high-throughput alternative to active focusing methods that require an external force-field to manipulate particles. In this study, we introduce inertial microfluidics in flows through straight, multiple parallel channels. The scalable, single inlet and two outlet, parallel channel system is enabled by a novel, high-density 3D PDMS microchannel manufacturing technology, mediated *via* a targeted inhibition of PDMS polymerization. Using single channels, we first demonstrate how randomly distributed particles can be focused into the centre position of the channel in flows through low aspect ratio channels and can be effectively fractionated. As a proof of principle, continuous focusing and filtration of 10 μm particles from a suspension mixture using 4- and 16-parallel-channel devices with a single inlet and two outlets are demonstrated. A filtration efficiency of 95–97% was achieved at throughputs several orders of magnitude higher than previously shown for flows through straight channels. The scalable and low-footprint focusing device requiring neither external force fields nor mechanical parts to operate is readily applicable for high-throughput focusing and filtration applications as a stand-alone device or integrated with lab-on-a-chip systems.

Introduction

Inertial induced forces in microchannels have recently received attention as a promising approach for particle focusing, filtration and separation.[1–9] In inertial microfluidics, wall- and shear-induced lift forces dominate and cause particles to move across streamlines and occupy equilibrium positions along the faces of channel walls. Across-channel migration of particles due to inertial lift forces was first experimentally shown by Segré and Silberberg.[10] They showed that particles in Poiseuille flow in a cylindrical pipe of radius R migrated to an equilibrium position located at $r = 0.62\ R$ for small Reynolds numbers (Re). For increased values of Re, the equilibrium position was found to move towards the wall. In these systems, the parabolic velocity profile results in a shear gradient-induced lift force on particles, which is directed down the shear gradient towards the wall, and a wall-induced lift force, directed away from a stationary wall. The resulting force field moves particles to a channel cross-sectional equilibrium position. For small particles ($R_p \ll 1$), the resulting balancing lift force, F_L, has been shown to scale with the particle Reynolds number squared (R_p^2) and a lift coefficient (fc):[11] $F_L = fc\ R_p^2\ \mu^2/\rho$, in which $R_p = (\mathrm{Re}(a/D_h)^2)$ is the particle Reynolds number. R_p depends on the intrinsic properties of the fluid, described by the channel Reynolds number, Re ($=\rho U_m D_h/\mu$), on the particle diameter (a) and on the hydraulic diameter ($D_h = 2wh/(w + h)$, for rectangular cross-section, w and h being the width and height of the channel). U_m is the maximum channel velocity; μ and ρ are the viscosity and density of the fluid, respectively.

Recently, lateral particle migration was extended to microfluidic channels, and it has been shown that particles can be focused in four points along the centre of wall faces for flow through microchannels with square ($50 \times 50\ \mu m^2$) cross-section.[1] While different curved geometries have been explored to reduce the cross-sectional focusing positions, including asymmetrically repetitive curves[3] and spirals,[7] much can be achieved with straight channels by simply reducing the aspect ratio (AR) of the cross-section. Recently, a straight, high aspect ratio ($20 \times 50\ \mu m^2$) microchannel was used to continuously focus and filter particles based on size,[4] in which particles were focused along the face of the longer channel sidewalls, generating two symmetric focusing points. However, for filtration applications and particle counting a single focused particle stream seen from top view is desired. In this paper, we explore particle focusing in flows through straight channels where the channel AR is varied towards low AR ($h < w$) for applications in high-throughput particle filtration.

One of the most promising applications for microfluidics is clinical diagnostics, with point-of-care blood processing being at the forefront. However, practical applications, such as isolation of micro-organisms from whole blood for sepsis diagnostics and

[a]*Division of Cell Physics, Department of Applied Physics, Royal Institute of Technology, Stockholm, Sweden. E-mail: aman@kth.se; Fax: +46-8-55378216; Tel: +46-8-55378343*
[b]*Division of Nanobiotechnology, KTH Royal Institute of Technology, Stockholm, Sweden*
[c]*Microsystem Technology Lab, KTH Royal Institute of Technology, Stockholm, Sweden*
[d]*Science for Life Laboratory, Stockholm, Sweden*

rare circulating tumour cells for cancer diagnostics, often require processing large volumes of blood ($\sim$5–10 ml). To meet the need for large volume sample processing, while simultaneously precisely and reliably sorting blood constituents, parallelized microfluidic channels are well suited. While relatively high volumetric flow rates can be accomplished in flow through spiral channels,[7] it is difficult to parallelize the channels. Although a ring format design was able to reduce the number of outlets in flow through straight parallel channel devices by merging the side outlets to form a ring,[12] parallelization traditionally results in a multiplication of the number of outlets, which makes fractional sample collection cumbersome. To minimize downstream sample handling, the sorting device should, ideally, contain only one sample inlet and one outlet for each sorted fraction. For parallelized devices, where sorting is performed simultaneously in many channels, streams must be able to pass each other without mixing, in order to collect each fraction in a single dedicated outlet. Only 3D microfluidic devices, with vertical channel connections (vias), are able to fulfil this demand.

Several methods for the formation of 3D channels in PDMS have been developed,[13–17] though these methods are typically unpractical and of low yield and repeatability. To counter these problems, a technique using dual level molds was developed in our lab.[18] This technique relies on the polymerization inhibition of PDMS at positions where fluidic vias are required: the PDMS prepolymer is poured onto the dual level mold, where the highest mold level defines the vias and the lower mold level defines the channel system. The polymerization inhibition is caused by an amine layer, coated on a glass plate that is clamped onto the higher level of the mold during curing. While 25 mm^2 devices were easily achievable using this technique, larger surface areas, as needed for inertial focusing devices, were found hard to manufacture due to excessive adhesion between the stiff glass top plate and the cured PDMS layer.

We here improve our previous method by using a flexible transfer foil, rather than a stiff glass plate, for the inhibition. We successfully demonstrate the reliable production of single inlet, scalable parallel-channel, and two outlet inertial devices using densely packed PDMS-vias by employing direct coupling of the inhibiting silane to a flexible polycarbonate foil. We first evaluated particle focusing behaviour in flows through single channels and report on how particles can be focused into four or two focusing points depending on particle Reynolds number, Rp. Finally, we utilized the novel technique to fabricate large area 3D microfluidic devices for high throughput particle sorting. As a proof of principle, continuous focusing and high throughput filtration of particles is demonstrated in 4- and 16-parallel-channel systems.

Materials and methods

Design

For studies of inertial particle focusing we designed devices containing straight 30 mm long, single layer channels with four different rectangular cross sections: 30 $\times$ 80 μm^2, 50 $\times$ 50 μm^2, 50 $\times$ 100 μm^2 and 50 $\times$ 250 μm^2.

For high throughput particle filtration we designed a two layer PDMS microfluidic device with multiple parallel straight channels interconnected through vias. Each channel is 20 mm long. The first 10 mm channel length had a cross-section of 30 $\times$ 80 μm, after which a tapering of the width begins and reaches 160 μm at a trifurcating exit in order to increase particle resolution. The middle fraction of the flow is distributed through a 3D microfluidic network with vias connecting to the top PDMS layer (outlet 1, see Fig. 1h for layout), while the two side fractions exit through side channels that are re-combined in the bottom PDMS layer (outlet 2, see Fig. 1b for layout). The top PDMS layer contains features to facilitate manual alignment and the fluidic resistance was chosen to collect about one fourth of the sample in the middle fractions of the channels (outlet 1). Two different multiple parallel channel designs (4 and 16) were fabricated and evaluated.

Fabrication

SU8-silicon molds were fabricated using standard lithography techniques. For the single layer, single channel PDMS devices, SU8 molds with heights of 30 μm and 50 μm were fabricated. For the two-layer parallel channel devices, two SU-8 molds, one single layer mold with the height of 30 μm for the top PDMS layer and one dual layer mold for the bottom PDMS layer were fabricated. For the dual layer mold, the bottom and the top SU8 layers were 30 μm, respectively 200 μm high. The molds were passivated with a fluorocarbon film formed through C_4F_8 plasma deposition.

PDMS prepolymer was prepared by mixing the PDMS at a standard 1 : 10 ratio (Sylgard 184, Dow Corning, USA) and degassing in a vacuum chamber. To produce the single layer channel, PDMS prepolymer was poured onto the SU-8 mold and cured at 65 °C overnight. The PDMS was then cut from the mold and three fluidic access ports were punched at the in- and outlets. Finally the PDMS was covalently bonded to glass slides using oxygen plasma (Femto, Diener, Germany) and heat-treated for 10 min on a 65 °C hotplate.

Fabrication of the multilayer parallel channel devices were performed in several steps (Fig. 1). First, an inhibition polycarbonate (PC) foil was prepared by incubating a flexible 250 μm thick PC foil (Packningar & Plast AB, Sweden) for one hour in a solution of 4% Pt inhibitor aminoethylaminopropyltrimethoxysilane (AEAPS, Z-6020, Dow Corning, USA) in methanol and baking for 10 min at 105 °C on a hotplate to create an amine surface coating (Fig. 1a) that inhibits PDMS polymerization. PDMS prepolymer was poured onto the dual layer bottom mold (Fig. 1c). The PC plate and a glass plate for structural support was clamped onto the prepolymer and cured for 30 min at 65 °C. During curing, the polymerization is locally inhibited on top of the highest mold features (*i.e.* the vias positions), as described in[18] and illustrated in Fig. 1d.

The polymerized PDMS adheres better to the PC foil than to the Teflon coated mold. Its flexibility allows the PC-PDMS stack to be peeled off from the mold (Fig. 1e). The bottom PDMS surface of the PC-PDMS stack is treated with oxygen plasma and bonded covalently to a clean and oxygen plasma treated glass slide (Fig. 1g). This ensures the adhesion between the PDMS and the glass to be higher than that between the PDMS and the PC. The flexible PC plate is thereafter peeled off from the PDMS-glass device. The unpolymerized PDMS residues at the *via* positions follow the PC plate, thus forming open vias in

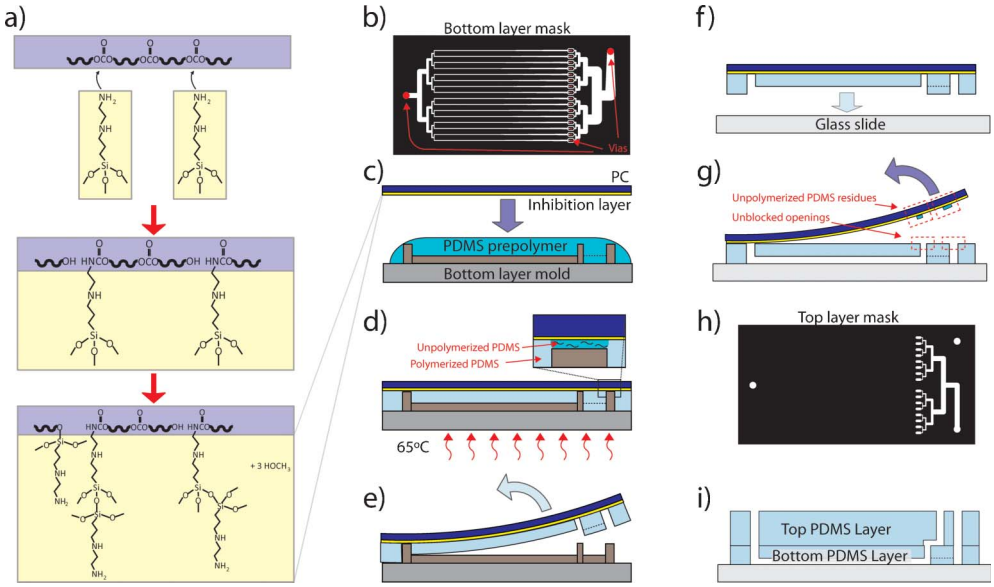

Fig. 1 Fabrication steps of a high throughput filtering device. (a) During the incubation step of the PC foil into 4% of Z-6020 the diamine silane binds to the polycarbonate in two distinct stages. (b) Bottom layer mask design used to produce bottom layer mold. Vias positions marked in red are used in a second mask to define higher mold features. (c) The PC inhibition foil is applied onto the PDMS prepolymer and clamped to the bottom layer mold. (d) During baking, the thin layer of PDMS close to the inhibition layer remains unpolymerized, whereas the bulk polymerizes. (e) The flexibility of the PC plate allows the PC-PDMS stack to be peeled of the mold. (f) The PC-PDMS sheet is transferred and plasma-bonded to a glass plate. (g) The PDMS sticks to the glass as the PC plate is peeled off, leaving unpolymerized PDMS residues on the PC-plate and unblocked openings in the PDMS layer. (h) Top layer mask used to produce top layer mold and casting the thick top PDMS layer. (i) The second, thicker PDMS layer is aligned and plasma-bonded on top of the bottom PDMS.

the PDMS (Fig. 1g). The top PDMS layer (see Fig. 1h for design) is prepared from the second, single layer SU8 mold and is, after hole punching and oxygen plasma treatment (15 s at 40 W, FEMTO A, Diener electronic GmbH), manually aligned and bonded to the bottom PDMS layer (Fig. 2g). The bond is cured for 10 min at 65 °C on a hotplate. Using this method, 4-, and 16-parallel channel devices were fabricated.

Experimental setup

The device characterization is based on the analysis of fluorescent microspheres flowing through the channels. Internally dyed green and red fluorescent polystyrene microspheres (2, 5, 8, 10, and 15 μm in diameter, Thermo Scientific) were diluted to 0.1–0.5 vol % with deionized water with 0.1% TritonX-100 (BDH Prolabo). The solutions were pumped by a syringe pump (Harvard Apparatus PHD 2000, Harvard Apparatus, USA) connected by tubing to the inlet of the PDMS devices. The device was mounted onto the stage of an inverted fluorescent microscope and fluorescent streak images were obtained. For single channel focusing studies, various flow rates and microspheres were tested for each channel and florescent microscopy images were acquired at 1, 10, 20 and 30 mm distance from the inlet. For filtration characterization, a suspension mixture of 10 μm (green) and 2 μm (red) microspheres was pumped through the multilayer (4- and 16-parallel channel) devices and the particle fractions collected at the two outlets (outlet 1 and 2) were quantified by a coulter counter (Z2, Beckman Coulter, USA). Additionally, pressure measurements were performed by connecting a pressure gauge close to the inlet of the device while pressing fluid through the devices at specific flowrates.

Image analysis

The fluorescent images were cropped and the pixel intensities were processed. The baselines of the intensities were corrected to be zero outside the channel and the widths were normalized by setting the x-positions of the walls to 0 and 1 respectively. The intensities were normalized and the resulting graphs were plotted (Fig. 2 b–d).

Result and discussions

Inertial focusing

Inertial migration of particles across streamlines in microchannels has been the subject for a number of studies.[1,5,19] The inertial lift force, F_L, varies in magnitude across the channel cross-section, which leads to difficulties of predictions, though a recent study has addressed this to some extent.[20] In previous work, it has been shown that square channels focus particles to four equilibrium positions,[1] while rectangular channels focus particles to two positions, each centered upon the faces of the channel's long walls.[4] In this study, we show that particles can be focused both into four and two points in flows through rectangular cross-sections (Fig. 2). Fig. 2a illustrates a summary of particle behaviour in flow through different aspect ratio (AR 1 : 1; 1 : 2, 1 : 3 and 1 : 5) microchannels. The different aspect ratios were obtained by fabrication of 30 × 80 μm^2, 50 × 50 μm; 50 × 100 μm^2 and 50 × 250 μm^2 microchannels. For AR 1 : 1, particles are focused along the faces of all walls, in agreement with previous work.[1] As the AR is decreased ($h < w$), several observations can be made. First, the larger the particle, the better focusing is obtained (Fig. 2b). This is expected since the lift force

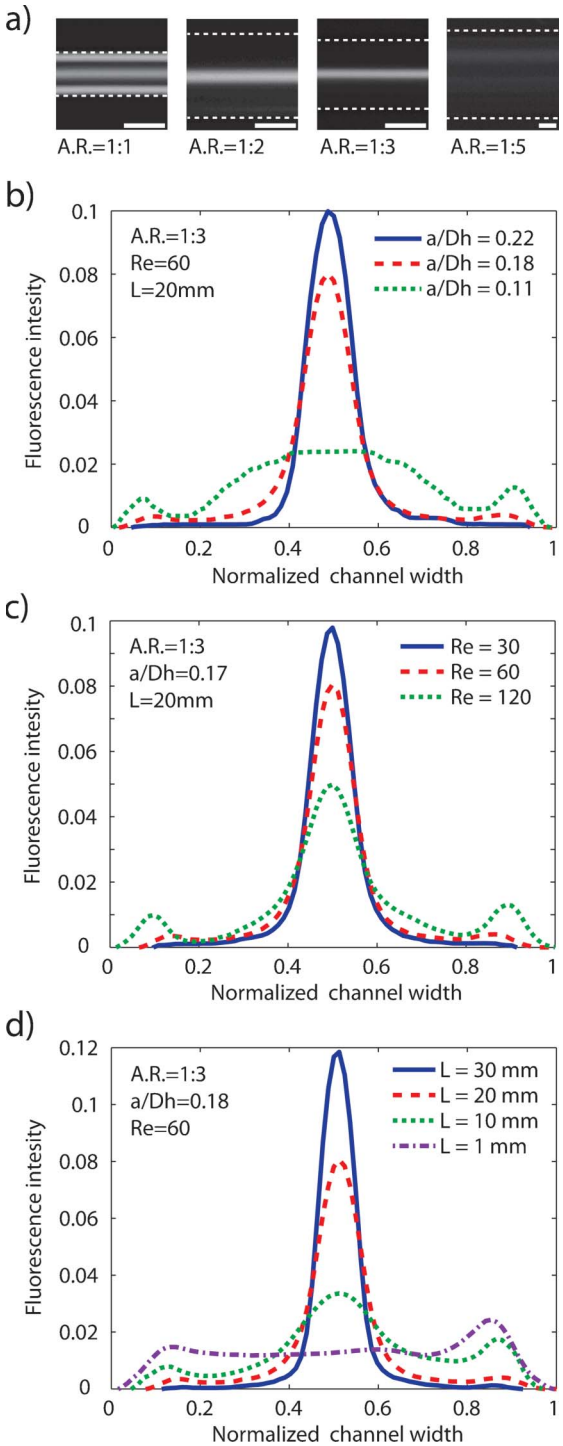

Fig. 2 Particle focusing in flow through single channels. (a) Fluorescence images of particle streams in channels of different aspect ratios (AR) taken at L = 20 mm. The channel Reynolds numbers are, from left to right: 51, 51, 61 and 56 and the particle to channel geometry ration, a/D_h: 0.20, 0.23, 0.23 and 0.12. The white dotted lines indicate the position of the wall. Scale bars: 50 μm. (b–d) Intensity plots of particle stream images with varying particle size to channel geometry ratio, a/D_h (b); Re (c); and channel length, L (d).

is proportional to the fourth power of particle size (F_L proportional a^4). For a low AR rectangular geometry, the lift force along the dimension defined by the channel height is dominant and it is expected that particles will tend to focus into two laterally broad focusing positions (top and bottom of the rectangular channel). However, as can be seen in Fig. 2b, the combination of channel AR and particle size to channel geometry ratio (a/D_h) affect where along the channel cross-section a particle will be focused. The larger particles ($a/D_h > 0.2$) are predominantly focusing at a two positions at the channel centre, while smaller particles are lagging behind and tend to focus in four focusing positions. A recent study in flow through channels with square cross section suggests a gradual transition from the lateral tubular pinch (forcing the particles to a ring like formation) to the cross-lateral focusing (forcing the particles along the ring to the four focusing positions) with increasing Re [19]. Similarly, particles in flow through low AR might first migrate to the lateral equilibrium positions (ellipse like formation), and then cross-laterally to the attractors at the centre faces of each wall. As the lift force is proportional to the fourth power of particle size, it is then possible to differentially focus larger particles (higher Rp) at the centre faces of the longer wall while smaller particles remain at the lateral equilibrium positions. In other words, inertial migration of larger particles is fully developed faster (*i.e.* at shorter channel length) compared to smaller particles. This means that given enough length and speed, smaller particles above a critical size (a/Dh > 0,07) would also migrate and occupy a two positions for flows through low AR microchannels.

To investigate the effect of Re in flows through low AR microchannels in detail, 8 μm particles (a/D_h = 0.17) were flown at different flow rates (Fig. 2c). As discussed above, moderate Re ($0.6 < R_p < 2.4$) resulted in particle migrations cross-laterally towards the two central equilibrium positions. Interestingly, when the flow rate is too high, some of the particles are not able to leave the centre face of the smaller wall within the channel length resulting in four focusing positions. In Fig. 2c, this effect is clearly seen for the higher flow rate (Re = 120). One possible explanation is that the shear rate along the smaller channel wall becomes significant to trap particles at the centre wall positions when Rp is significantly increased. Similar results were obtained for other particle sizes. In addition, we investigated the effect of channel length for a given Re (Fig. 2d). Already after 10 mm, the particles start to focus at broader equilibrium positions. While moving downstream, the particles migrate cross-laterally towards the centre. Once the particles reach the centre, they remain at the focusing position. Although more investigation will be required to fully understand the physics behind the focusing phenomena, our experimental observations suggest it is possible to use the particle size with respect to channel dimensions and the defined flow parameters to differentially focus particle of different sizes at different positions within the channel cross-section. For particle filtration applications, size dependent particle migration towards attractors at the two central positions might open the possibility to passively filter particles with small size difference.

Multilayer parallel-channel devices

In the inhibition technology previously developed in our lab, a glass plate was used as the top in the mold set-up. While through holes were easily produced, the strong adhesion between the plate and PDMS made delamination very difficult for large area devices. Intermittently, the PDMS even ruptured during this process step. Since parallelization invariably increases the device surface, the size restriction inherent in the previous technique was clearly impermissible in this work. To counter delamination problems, we developed a protocol using a 250 μm thick polycarbonate (PC) foil which is flexible enough for easy separation of the plate and the inhibited PDMS layer (Fig. 1). For structural support of the flexible PC foil we used a glass plate during curing. This has enabled us to successfully transfer PDMS structures with areas of 50 to 1000 mm^2. Fig. 3a shows the PDMS vias in a 16-parallel-channel design. The yield of the vias formation was repeatedly 100% in all the devices fabricated. As can be seen in Fig. 3b–d, we were able to reliably produce scalable parallel-channel inertial focusing devices.

The mode of reaction between the silane inhibitor and a glass surface used previous is different from the reaction between the silane inhibitor and polycarbonate. The former proceeds *via* condensation reactions between surface bound hydroxyl groups on the glass and the silane functional group resulting in a covalent SiO link upon expulsion of an alcohol molecule. In contrast, with this simple one step process, the reaction between polycarbonate and a diamine silane proceeds in two distinct stages: firstly, a chain breaking reaction between the polycarbonate chain and a primary amine occurs, resulting in a polymer surface that contains covalently bound hydroxyl groups and silane groups; secondly, the hydroxyl and silane groups both take part in a condensation reaction with a second inhibitor silane molecule (see Fig. 1a). The dual stage reaction does not require a two-step process since the diamine silane functions both as a linker with the polycarbonate and as an inhibitor of PDMS polymerization.

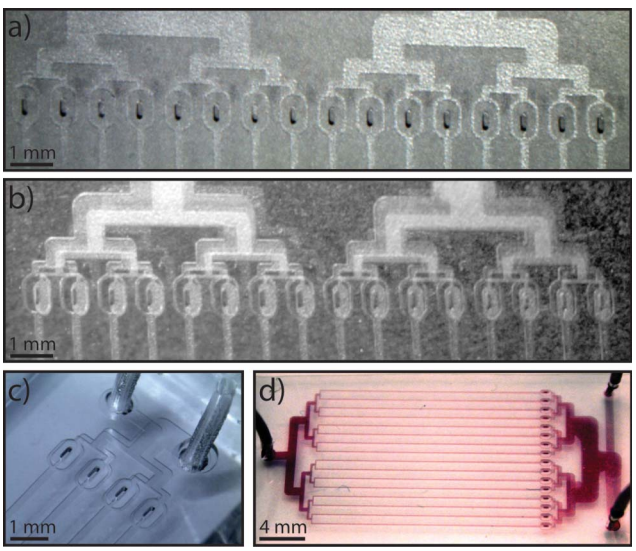

Fig. 3 Multilayer parallel-channel device fabrication. (a) A close-up photo of the bottom layer of a 16-parallel-channel PDMS device with open vias. (b) A 16-parallel channel, two-layer PDMS, interconnected through vias. The top PDMS layer is aligned and bonded onto the bottom PDMS layer. (c) A 4-parallel-channel, two-layer PDMS showing the 3D-fluidic network leading to the two separate outlets. (d) A 16-parallel-channel filtration device filled with red dye. The distance from the inlet to the outlets is 32 mm and the total footprint area of the device is less than 550 mm^2.

High throughput particle filtration

Based on the focusing results using single channel devices, we fabricated parallel-channel devices with channel cross-sections of 30×80 μm^2. In order to enhance resolution of the streams at the outlets, the cross-section is tapered to a total width of 160 μm after 10 mm over length of another 10 mm, adding up to a total channel length of 20 mm. The centre fractions are processed through the vias and the parallel channels are reconnected in the second PDMS layer and collected (outlet 1, in Fig. 4a), while the

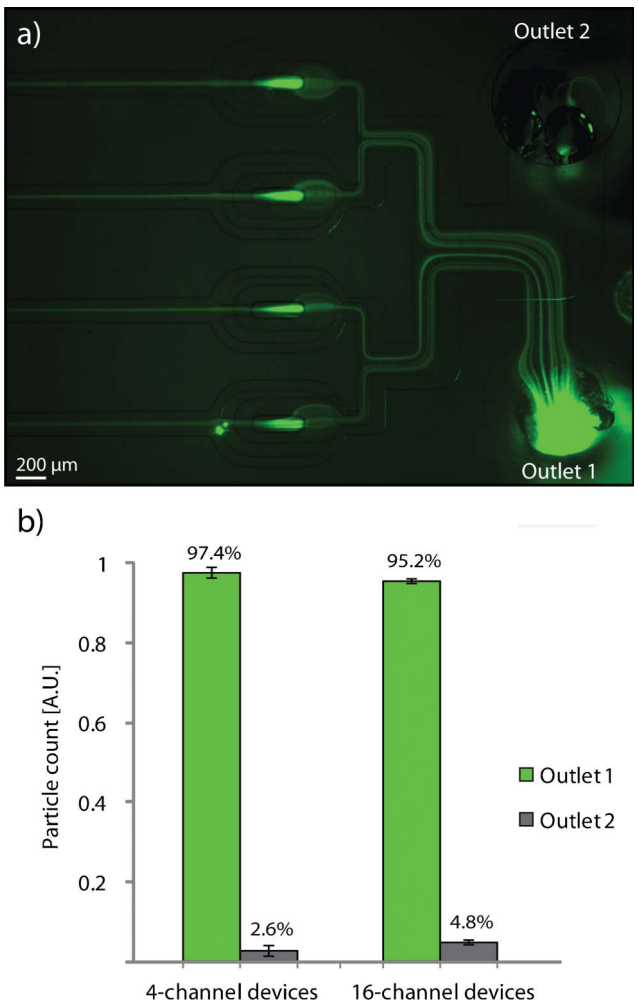

Fig. 4 High-throughput filtration. (a) Inverted fluorescence image of a 4-parallel-channel device showing filtration of 10 μm particles. The particles are focused at the centre streamline that enters the middle fraction and are collected in the top PDMS layer and exits through outlet 1. Flow rate: 0.8 mL min^{-1}. (b) Filtration of 10 μm particles from a mixture containing 10 and 2 μm particle flown through 4-,and 16-parallel channel devices. A filtration efficiency of 97.2%, and 95.3% was obtained for the 4-, and 16-parallel channel devices respectively. The flow rates were 0.8 ml min^{-1}, and 3.2 ml min^{-1} for respective devices.

side streams remain in the first PDMS layer and are collected through outlet 2. Since the particles are focused at the central positions, the flow resistance design of the different outlet channels was balanced to collect a smaller volumetric fraction through outlet 1. For the 4-parallel-channel devices, the volumetric fraction was measured to 25%, while for the 16-channel device the corresponding fraction was 28%. A mixture of 10 μm and 2 μm particles was pushed through the devices. The 10 μm particles were focused and could be successfully fractionated through outlet 1 (Fig. 4a). As expected, the 2 μm particles remained unfocused. The filtration efficiency of the 10 μm particles was in the range of 95–97% for the two multichannel devices, as analyzed with a coulter counter (Fig. 4b). The flow rates, 0.8 and 3.2 ml min^{-1} for the 4- and 16-parallel channel devices respectively, were chosen to match the results from single channel devices, where 200 μl min^{-1} was found to be optimal for focusing of 10 μm particles. At these flowrates the pressure drop over the devices were measured to around 2.5 Atm. The high filtration efficiency for both 4 and 16 parallel channels indicates that the focusing principle is highly scalable. Furthermore, to test the robustness of the system, a 16-channel device was tested for filtration at flow rates from 0.8 to 4 ml min^{-1}. In all cases the filtration efficiency for the 10 μm particles were >90% (Fig. 5). The effective filtration under large range of flow rates stem from the fact that particles start the migration towards the centre focusing position at low Re and are maintained focused under a relatively large Re before defocusing (Fig. 5a). The large range of Re under which particles are focused makes the system robust against flow fluctuations. Compared to other microfluidic systems, the parallel-channel deceives can therefore tolerate fabrication defects and clogging in one or more of the channels since the fluid would be evenly distributed throughout the remaining channels as long as the Re at each channel is sufficient to focus particles. Other continuous flow separation techniques include active separation techniques that uses externally induced forces such as magnetic,[21] optical[22] or acoustic[23] generally resulting in high separation specificity, low flowrates, and requiring more advanced equipment such as actuators *etc.*, and passive separation techniques relying on channel design and geometry for particle separation *e.g.* deterministic lateral displacement,[24] pinched flow fraction.[25] Compared to these systems, inertial microfluidics uses the highest volumetric flowrates, even in single channels. A drawback with our system is, however, it is limited to large volume samples since it require relatively high Reynolds number to operate.

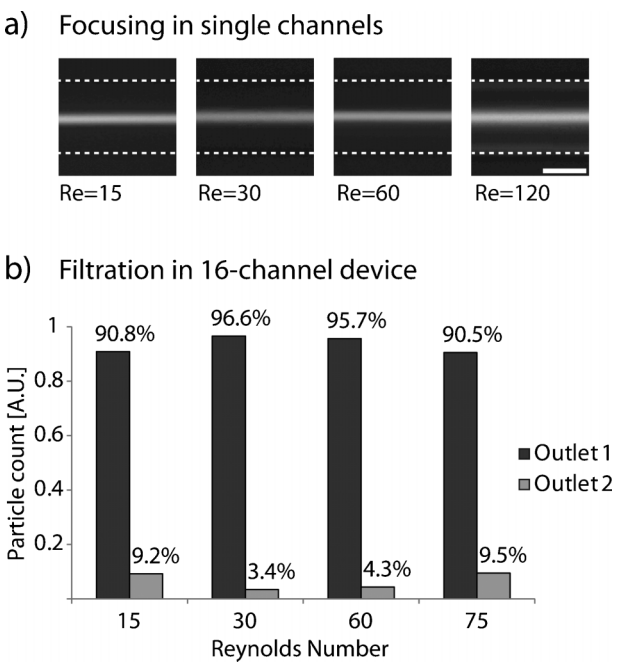

Fig. 5 Robustness to change in flowrate. (a) Fluorescence microscopy images of 10 μm particle streams at different flowrates corresponding to Reynolds numbers of 15, 30, 60 and 120. The channels have a height of 30 μm and a width of 80 μm and the images are taken at L = 20 mm. The white dotted lines indicate the position of the wall. Scale bars: 50 μm. (b) Filtration of 10 μm particles at different Re in flow through a 16-parallel-channel device. The corresponding volumetric flow rates are, from left to right: 0.8; 1.6; 3.2; and 4 mL min^{-1}. The filtration efficiency was >90% for all the flow rates.

Biological processes involving complex fluids, such as blood, often require preparative separation for the subsequent procedures. Conventional centrifugation techniques are among the most widely used methods for cell separation, which exploit differences in size and density. Although high throughput (handles typically mL blood volumes), it takes relatively long periods of hands-on time, and often requires bulky, mechanically complex apparatus to achieve the desired separation or enrichment. In this study, we have shown particle filtration in flow through 16 parallel channels with flow rates up to 4 mL min^{-1} with maintained high (>90%) efficiency, a throughput comparable to macroscale filtration. More important, the scalable, one-inlet and two-outlet, design allows continuous flow sample preparation, with minimal manual handling and is readily applicable as standalone device or integrated into lab on a chip systems.

In this paper we use rigid polystyrene microsphere as a model for inertial focusing. Future work will include applications in cell separation. The validity of polystyrene particles as a model for cells has previously been discussed.[12,26] It has been shown that non-rigid particle[26] and non-spherical cells[26] focus at a slightly different distance from the channel wall compared to rigid spherical particles. Although, this difference should not affect the filtering capacity of this device since the focusing position in low AR microchannel is independent of where the cells are along the height of the channel, the geometry (channel width, height and length) will have to be optimized for cell separation applications.

Conclusions

In summary, we report inertial focusing in flows through straight channels with rectangular low AR cross-section geometries and show how particles can be focused into two or four focusing points, depending on size, channel geometry and length. Using a novel 3D vias production scheme for large area devices, we fabricated leak-tight, parallel channel microdevices with only two outlets for simple downstream integration. We report filtration efficiency of 95–97% at high ($\sim$ml min^{-1}) throughputs. Finally, the novel method introduced in this paper allow scalable and easy to integrate parallel-channel inertial filtration devices

offers the key advantage of processing large volumes and could be useful for a range of applications in which sample needs to be processed rapidly.

Acknowledgements

This work has been sponsored in part by the European Commission through the projects FP7 InTopSens and IMI RAPP-ID.

References

1 D. Di Carlo, D. Irimia, R. G. Tompkins and M. Toner, *Proc. Natl. Acad. Sci. U. S. A.*, 2007, **104**, 18892–18897.
2 J. Seo, M. H. Lean and A. Kole, *J. Chromatogr., A*, 2007, **1162**, 126–131.
3 D. Di Carlo, J. F. Edd, D. Irimia, R. G. Tompkins and M. Toner, *Anal. Chem.*, 2008, **80**, 2204–2211.
4 A. A. S. Bhagat, S. S. Kuntaegowdanahalli and I. Papautsky, *Phys. Fluids*, 2008, **20**, 101702.
5 A. A. S. Bhagat, S. S. Kuntaegowdanahalli and I. Papautsky, *Microfluid. Nanofluid.*, 2008, **7**, 217–226.
6 A. A. S. Bhagat, S. S. Kuntaegowdanahalli and I. Papautsky, *Lab Chip*, 2008, **8**, 1906.
7 A. Russom, A. K. Gupta, S. Nagrath, D. D. Carlo, J. F. Edd and M. Toner, *New J. Phys.*, 2009, **11**, 075025.
8 Z. Wu, B. Willing, J. Bjerketorp, J. K. Jansson and K. Hjort, *Lab Chip*, 2009, **9**, 1193.
9 D. Di Carlo, *Lab Chip*, 2009, **9**, 3038.
10 G. Segré and A. Silberberg, *Nature*, 1961, **189**, 209–210.
11 E. S. Asmolov, *J. Fluid Mech.*, 1999, **381**, 63–87.
12 A. J. Mach and D. Di Carlo, *Biotechnol. Bioeng.*, 2010, **107**, 302–311.
13 J. R. Anderson, D. T. Chiu, R. J. Jackman, O. Cherniavskaya, J. C. McDonald, H. Wu, S. H. Whitesides and G. M. Whitesides, *Anal. Chem.*, 2000, **72**, 3158–3164.
14 B.-H. Jo, L. M. Van Lerberghe, K. M. Motsegood and D. J. Beebe, *J. Microelectromech. Syst.*, 2000, **9**, 76–81.
15 Y. Nam, K. Musick and B. C. Wheeler, *Biomed. Microdevices*, 2006, **8**, 375–381.
16 Y. Luo and R. N. Zare, *Lab Chip*, 2008, **8**, 1688.
17 J. H. Kang, E. Um and J.-K. Park, *J. Micromech. Microeng.*, 2009, **19**, 045027.
18 C. F. Carlborg, T. Haraldsson, M. Cornaglia, G. Stemme and W. van der Wijngaart, *J. Microelectromech. Syst.*, 2010, **19**, 1050–1057.
19 Y.-S. Choi, K.-W. Seo and S.-J. Lee, *Lab Chip*, 2011, **11**, 460.
20 D. Di Carlo, J. Edd, K. Humphry, H. Stone and M. Toner, *Phys. Rev. Lett.*, 2009, **102**(9).
21 N. Pamme and A. Manz, *Anal. Chem.*, 2004, **76**, 7250–7256.
22 M. M. Wang, E. Tu, D. E. Raymond, J. M. Yang, H. Zhang, N. Hagen, B. Dees, E. M. Mercer, A. H. Forster, I. Kariv, P. J. Marchand and W. F. Butler, *Nat. Biotechnol.*, 2004, **23**, 83–87.
23 A. Lenshof, A. Ahmad-Tajudin, K. Järås, A.-M. Swärd-Nilsson, L. Åberg, G. Marko-Varga, J. Malm, H. Lilja and T. Laurell, *Anal. Chem.*, 2009, **81**, 6030–6037.
24 S. H. Holm, J. P. Beech, M. P. Barrett and J. O. Tegenfeldt, *Lab Chip*, 2011, **11**, 1326.
25 M. Yamada, M. Nakashima and M. Seki, *Anal. Chem.*, 2004, **76**, 5465–5471.
26 S. C. Hur, N. K. Henderson-MacLennan, E. R. B. McCabe and D. Di Carlo, *Lab Chip*, 2011, **11**, 912.

